Results in Physics 10 (2018) 385–390

Contents lists available at ScienceDirect

Results in Physics

journal homepage: www.elsevier.com/locate/rinp

Analytical solutions of photo-thermo-elastic waves in a non-homogenous semiconducting material

Aatef Hobiny[a], Ibrahim A. Abbas[a,b,*]

[a] Nonlinear Analysis and Applied Mathematics Research Group (NAAM), Department of Mathematics, King Abdulaziz University, Jeddah, Saudi Arabia
[b] Department of Mathematics, Faculty of Science, Sohag University, Sohag, Egypt

ARTICLE INFO

Keywords:
Photothermal theory
Plasma waves
Eigenvalue approach
Laplace transformation

ABSTRACT

In the present paper, the wave propagation on non-homogenous semiconductor through photo-thermal process has been studied by using the theory of coupled plasma and thermoelastic wave. Without neglecting the coupling between the plasma and thermoelastic wave that photo-generated through intensity modulated laser beam and tightly focused, a semiconducting isotropic elastic medium has non-homogeneity in thermal and elastic properties are considered. The analytical solutions in the domain of Laplace by the eigenvalues approach were observed through the transform techniques of Laplace. Silicon-like semiconductor was used to achieve the numerical computations.

Introduction

Essentially, considering qualitatively what happen when a laser beam with energy E was an incident on a semiconducting material that has forbidden gap of width E_g? If $E > E_g$ an electron will be traveled the valence band to an energy level of energy equals to $E{-}E_g$, above the conduction band edge. Then such electron or carrier will relax to one of the empty levels nearby the conduction band bottom namely non-radiative transition. relaxation process will be followed by the formation of hole-electron pairs through recombination. Electron and hole plasma will take place before recombination. The plasma density is controlled by the diffusion behavior which is the same of the heat flow of the thermal source. Thus, modulation of incident laser intensity behind the thermal wave, a modulated plasma density can be observed i.e., a plasma wave. In Semiconductors, an electronic deformation (ED) which is periodically malleable desaturation in material produced by the photoexcited carriers that may leads to locally strain in the material produces plasma waves. These waves behave as well as the thermal wave produced due to local periodic elastic desaturation.

Recently, the photoacoustic (PA) and photothermal (PT) methods were taken as diagnostic tools with high sensitivity to the electronic transport and thermal processes in microelectronic structures. Generally, semiconductor is characterized by its high electric resistivity that decreased by the increase of temperature. The semiconductor resistivity can be reduced by doping which is main in the design of semiconductor junctions. The behavior of charge carriers at the junction, is the main of manufacturing of diode, transistor, solar cells semiconducting detector and all modern solid state devices. Pure or intrinsic semiconductor such as Si is widely used in semiconducting industrial. Unlike metals the conduction in pure Si through electrons-holes and electrons that may be released from atoms within the crystal by thermal, and thus decrease silicon's electrical resistivity with higher temperatures.

Previously, Todorovic et al. [1–3] introduced an experimental and theoretical outcome on micro-mechanical structure of the thermoselastic and plasma fields. But, their study is restricted on one dimension (1D). Their theoretical analysis to describes the two phenomena that gives information about the properties of carrier recombination and transport in semiconductor. The effect of the electronic and thermoselastic deformation in semiconductor has been studied by [4–6] with neglecting the coupling the plasma and thermoelastic relations. When a probe beam was focused on the material surface there are local thermoelastic deformations due to the excitation [7,8]. On the other hand, Song et al. [9,10] study in detail, the thermoelastic vibrations of the photoexcited microcantilever. The photothermal and generalized thermoelastic theories were used to investigate the reflection of plane waves in a semiconductor medium [11,12]. Abbas [13] investigated the photothermal waves in a semiconductor material photogenerated by a focused laser beam. Abbas [14] studied the dual phase lag model on photo-thermal interactions in an infinite semiconducting media contain a cylindrical hole. Abbas and Aly [15] presented the generalized model on photo-thermal-elastic waves in a semiconducting medium. Abbas et al. [16] investigated the photo-thermal interaction in a semiconducting material under two-temperature theory.

* Corresponding author at: Nonlinear Analysis and Applied Mathematics Research Group (NAAM), Department of Mathematics, King Abdulaziz University, Jeddah, Saudi Arabia.
E-mail addresses: ahobany@kau.edu.sa (A. Hobiny), ibrabbas7@science.sohag.edu.eg (I.A. Abbas).

https://doi.org/10.1016/j.rinp.2018.06.035
Received 22 May 2018; Received in revised form 12 June 2018; Accepted 16 June 2018
Available online 27 June 2018

In the present paper, we attempt to study the analytical solutions of plasma-thermo-elastic waves photo-generated by a focused laser beam in a nonhomogeneous semiconducting material. Based on Laplace transform and eigenvalues approach, the dimensionless of basic equations are handled by employing an analytical–numerical technique. The numerical computations are made for silicon-like semiconducting material, and the outcomes are graphically represented.

Formulation of the problem

Generally, to understand the transport mechanism in a semiconductor considering simultaneously coupled of the plasma and the thermos-elastic waves their variables such as carriers density $n(\boldsymbol{r}, t)$, distribution of temperature $T^*(\boldsymbol{r}, t)$ as well as components of elastic displacement $u_i(\boldsymbol{r}, t)$. The photo-thermal theory in main based on three relationships for the motion, plasma and heat condition respectively [12,17]:

$$\sigma_{ij,j} = \rho\frac{\partial^2 u_i}{\partial t^2} \tag{1}$$

$$D_e N_{,jg} - \frac{N}{\tau} + \varepsilon T = \frac{\partial N}{\partial t} \tag{2}$$

$$(KT_{,j})_{,j} + \frac{E_g}{\tau}N - \gamma_t T_o\frac{\partial u_{j,j}}{\partial t} = \rho c_e\frac{\partial T}{\partial t} \tag{3}$$

The constitutive relations were written as:

$$\sigma_{ij} = \mu(u_{i,j} + u_{j,i}) + (\lambda u_{k,k} - \gamma_n N - \gamma_t T)\delta_{ij}, \tag{4}$$

where $i, j, k = 1, 2, 3$, $N = n - n_o$, n_o is the equilibrium carrier concentration, $T = T^* - T_o$, T_o is the reference temperature, σ_{ij} are the stress components, λ, μ are the Lame's constants, $\gamma_n = (3\lambda + 2\mu)d_n$, d_n is the coefficient of electronic deformation, ρ is the density of medium, u_i are the components of displacement, c_e is the specific heat at constant strain, $\gamma_t = (3\lambda + 2\mu)\alpha_t$, α_t is the linear thermal expansion coefficient, τ is the lifetime of the photogenerated carrier, $\boldsymbol{r}$ is the position vector, D_e is the carrier diffusion coefficient, t is the time, K is the thermal conductivity, and $\varepsilon = \frac{1}{\tau}\frac{\partial n_o}{\partial T}$ [17]. Now, we consider the problem of a semiconducting plane $z \geqslant 0$ and the state of the medium depends only on z and the time variable t. Therefore, Eqs. (1)–(4) can be rewritten as:

$$\frac{\partial \sigma_{zz}}{\partial z} = \rho\frac{\partial^2 u}{\partial t^2}, \tag{5}$$

$$D_e\frac{\partial^2 N}{\partial z^2} - \frac{N}{\tau} + \varepsilon T = \frac{\partial N}{\partial t}, \tag{6}$$

$$\frac{\partial}{\partial z}\left(K\frac{\partial T}{\partial z}\right) + \frac{E_g}{\tau}N - \gamma_t T_o\frac{\partial^2 u}{\partial t \partial z} = \rho c_e\frac{\partial T}{\partial t} \tag{7}$$

$$\sigma_{zz} = (\lambda + 2\mu)\frac{\partial u}{\partial z} - \gamma_n N - \gamma_t T, \tag{8}$$

In this study, we assume the non-homogeneous properties of the material are characterized by

$$\rho = f(z)\rho_o, \quad \mu = f(z)\mu_o, \quad \lambda = f(z)\lambda_o, \quad \gamma = f(z)\gamma_o, \quad E_g = f(z)E_{go}, \quad K = f(z)K_o, \tag{9}$$

where $f(z)$ is a continuous and non-dimensional function, $\rho_o, \mu_o, \lambda_o, \gamma_o, E_{go}$ and K_o are the values of $\rho, \mu, \lambda, \gamma, E_g$ and K in the homogeneous case, respectively. Substituting from Eq. (9) in Eqs. (6)–(8) can be obtain

$$\left(f(z)\frac{\partial}{\partial z} + \frac{\partial f}{\partial z}\right)\left((\lambda_o + 2\mu_o)\frac{\partial u}{\partial z} - (3\lambda_o + 2\mu_o)(d_n N + \alpha_t T)\right) = \rho_o f(z)\frac{\partial^2 u}{\partial t^2}, \tag{10}$$

$$D_e\frac{\partial^2 N}{\partial z^2} - \frac{N}{\tau} + \varepsilon T = \frac{\partial N}{\partial t}, \tag{11}$$

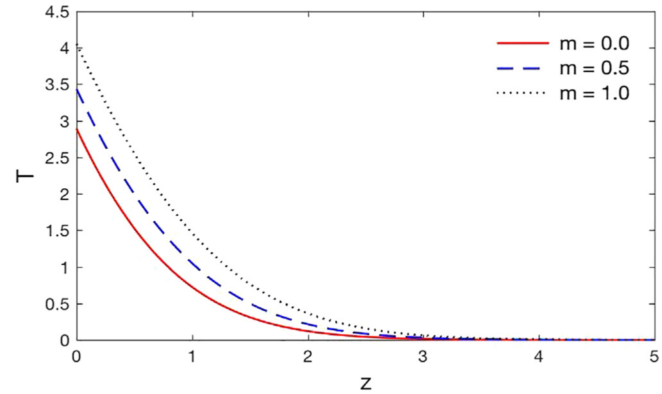

Fig. 1. The variation of temperature with the distance for different values of non-homogeneous parameter m case (i).

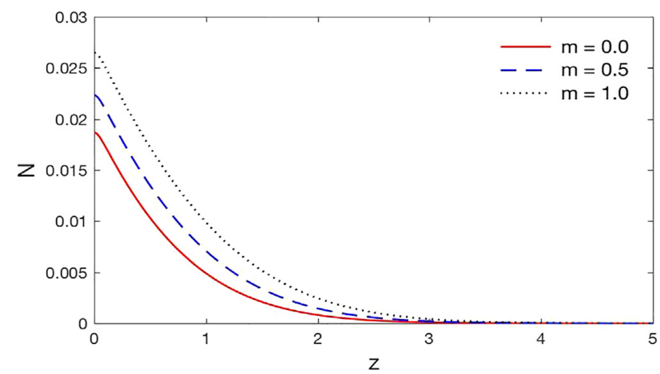

Fig. 2. The variation of carrier density with the distance for different values of non-homogeneous parameter m case (i).

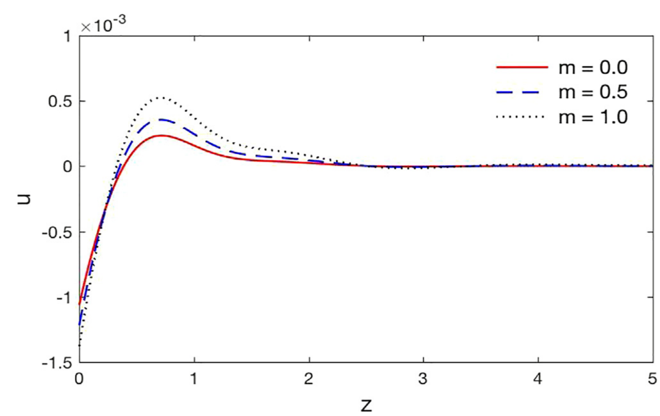

Fig. 3. The variation of displacement with the distance for different values of non-homogeneous parameter m case (i).

$$K_o\left(f(z)\frac{\partial}{\partial z} + \frac{\partial f}{\partial z}\right)\frac{\partial T}{\partial z} + \frac{E_{go}}{\tau}f(z)N - (3\lambda_o + 2\mu_o)\alpha_t T_o f(z)\frac{\partial^2 u}{\partial t \partial z} = \rho_o c_e f(z)\frac{\partial T}{\partial t} \tag{12}$$

$$\sigma_{zz} = f(z)\left((\lambda_o + 2\mu_o)\frac{\partial u}{\partial z} - (3\lambda_o + 2\mu_o)(d_n N + \alpha_t T)\right), \tag{13}$$

Applications

Initially, it must be considering the initial and boundary conditions. The initial conditions of the problem are assumed to be homogeneous and are supplemented by considering the boundary $z = 0$ is adjacent to

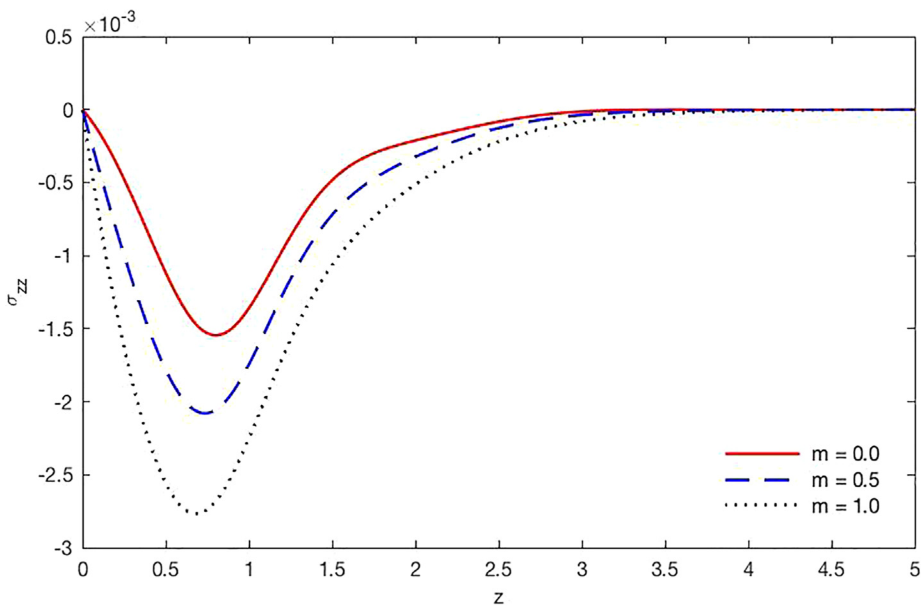

Fig. 4. The variation of stress with the distance for different values of non-homogeneous parameter m case (i).

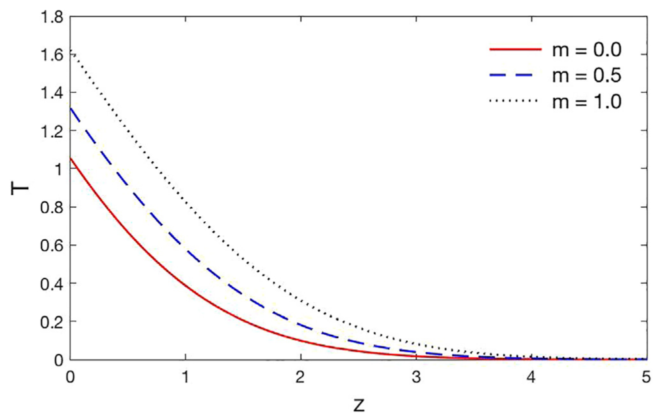

Fig. 5. The variation of temperature with the distance for different values of non-homogeneous parameter m case (ii).

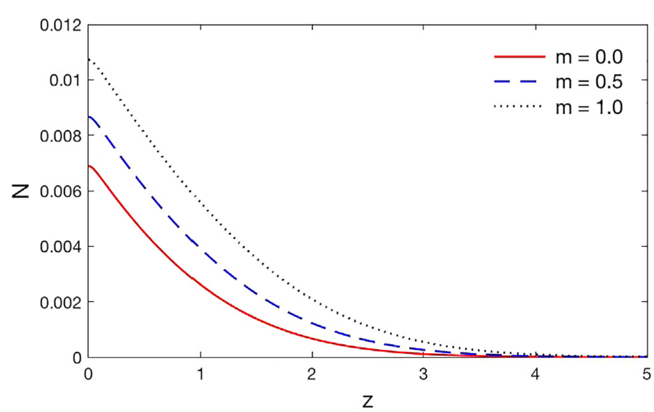

Fig. 6. The variation of carrier density with the distance for different values of non-homogeneous parameter m case (ii).

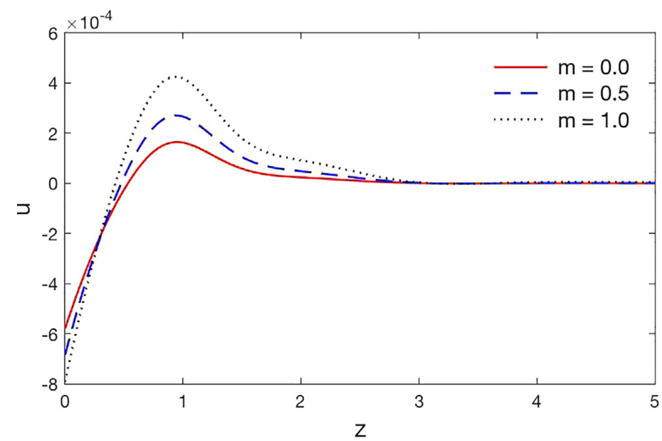

Fig. 7. The variation of displacement with the distance for different values of non-homogeneous parameter m case (ii).

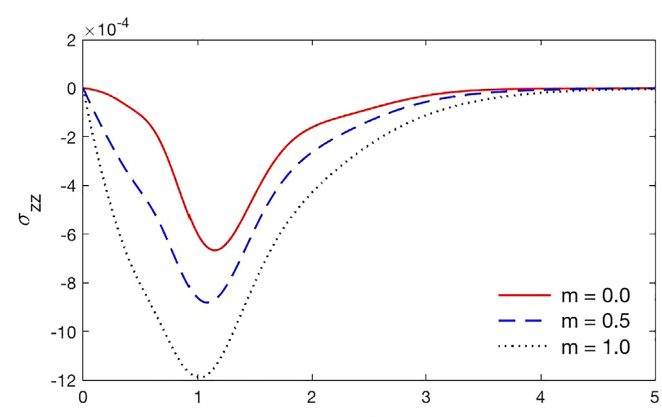

Fig. 8. The variation of stress with the distance for different values of non-homogeneous parameter m case (ii).

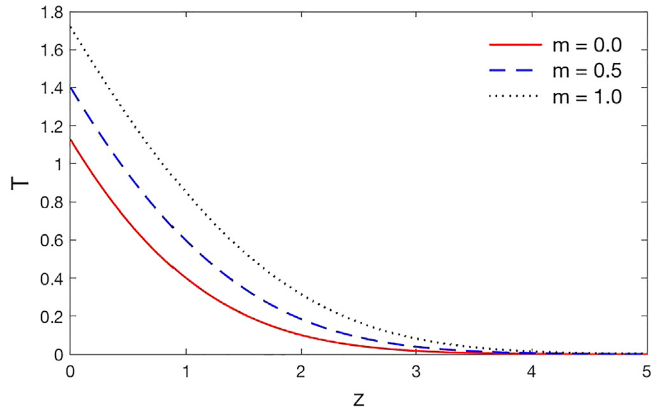

Fig. 9. The variation of temperature with the distance for different values of non-homogeneous parameter m case (iii).

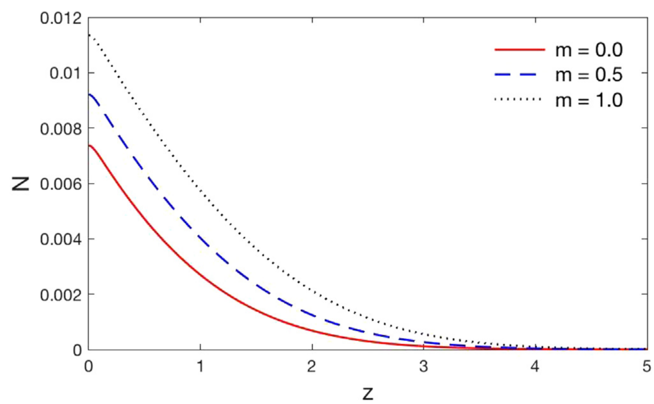

Fig. 10. The variation of carrier density with the distance for different values of non-homogeneous parameter m case (iii).

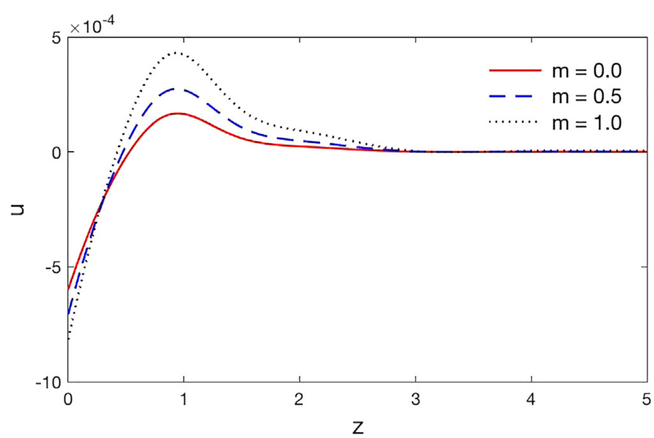

Fig. 11. The variation of displacement with the distance for different values of non-homogeneous parameter m case (iii).

vacuum. The boundary conditions can be considered by

Case (I): For $t>0$ the surface ($z=0$) is exposed to a laser-pulse heat flux and traction free, i.e.

$$-K\frac{\partial T(0,t)}{\partial z}=q_o\frac{t^2e^{-\frac{t}{t_p}}}{16t_p^2},\quad \sigma_{zz}(0,t)=0,\quad D_e\frac{\partial N(0,t)}{\partial z}=s_oN(0,t),\quad \frac{\partial T(\infty,t)}{\partial z}=0,\quad \sigma_{zz}(\infty,t)=0,\quad \frac{\partial N(\infty,t)}{\partial z}=0, \tag{14}$$

Case (ii): For $t>0$ the surface ($z=0$) is exposed to a transient cosine

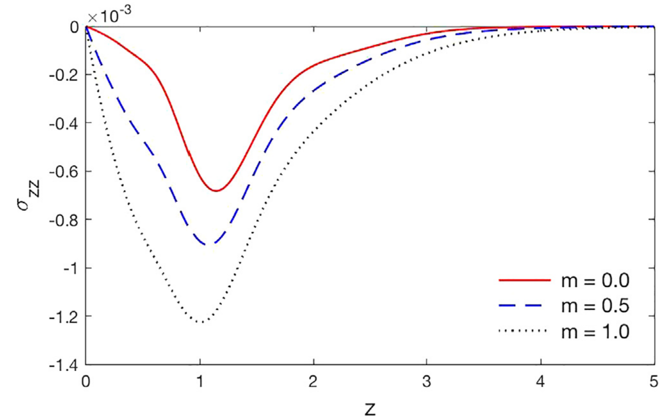

Fig. 12. The variation of stress with the distance for different values of non-homogeneous parameter m case (iii).

heat flux and traction free, i.e.

$$-K\frac{\partial T(0,t)}{\partial z}=q_o\cos(\omega t),\quad \sigma_{zz}(0,t)=0,\quad D_e\frac{\partial N(0,t)}{\partial z}=s_oN(0,t),\quad \frac{\partial T(\infty,t)}{\partial z}=0,\quad \sigma_{zz}(\infty,t)=0,\quad \frac{\partial N(\infty,t)}{\partial z}=0, \tag{15}$$

Case (iii): For $t>0$ the surface ($z=0$) is exposed to a constant heat flux and traction free, i.e.

$$-K\frac{\partial T(0,t)}{\partial z}=q_o,\quad \sigma_{zz}(0,t)=0,\quad D_e\frac{\partial N(0,t)}{\partial z}=s_oN(0,t),\quad \frac{\partial T(\infty,t)}{\partial z}=0,\quad \sigma_{zz}(\infty,t)=0,\quad \frac{\partial N(\infty,t)}{\partial z}=0, \tag{16}$$

where q_o is a constant, ω is the heating frequency, t_p is the pulse heat flux characteristic time and s_o is the velocity of surface recombinations. For conveniences, the dimensionaless varibles can be given as

$$T'=\frac{T}{T_o},\quad N'=\frac{N}{n_o},\quad (z',u')=\varsigma c(z,u),\quad \sigma'_{zz}=\frac{\sigma_{zz}}{\lambda_o+2\mu_o},\quad (t',\tau')=\varsigma c^2(t,\tau),\quad q'_o=\frac{q_o}{K\varsigma cT_o}, \tag{17}$$

where $c^2=\frac{\lambda_o+2\mu_o}{\rho_o}$, $\varsigma=\frac{\rho_oc_e}{K_o}$.

Canceled the primes and rewrite Eqs. (10)–(16) as follow:

$$\left(f(z)\frac{\partial}{\partial z}+\frac{\partial f}{\partial z}\right)\left(\frac{\partial u}{\partial z}-u_1N-u_2T\right)=f(z)\frac{\partial^2u}{\partial t^2}, \tag{18}$$

$$\frac{\partial^2N}{\partial z^2}-n_1\frac{N}{\tau}+\beta T=n_1\frac{\partial N}{\partial t}, \tag{19}$$

$$\left(f(z)\frac{\partial}{\partial z}+\frac{\partial f}{\partial z}\right)\frac{\partial T}{\partial z}+\frac{t_1}{\tau}f(z)N-t_2f(z)\frac{\partial^2u}{\partial t\partial z}=f(z)\frac{\partial T}{\partial t} \tag{20}$$

$$\sigma_{zz}=f(z)\left(\frac{\partial u}{\partial z}-u_1N-u_2T\right), \tag{21}$$

$$\frac{\partial T(0,t)}{\partial z}=-q_o\frac{t^2e^{-\frac{t}{t_p}}}{16t_p^2},\quad \sigma_{zz}(0,t)=0,\quad \frac{\partial N(0,t)}{\partial z}=\gamma N(0,t),\quad \frac{\partial T(\infty,t)}{\partial z}0,\quad \sigma_{zz}(\infty,t)=0,\quad \frac{\partial N(\infty,t)}{\partial z}=0, \tag{22}$$

$$\frac{\partial T(0,t)}{\partial z}=-q_o\cos(\omega t),\quad \sigma_{zz}(0,t)=0,\quad \frac{\partial N(0,t)}{\partial z}=\gamma N(0,t),\quad \frac{\partial T(\infty,t)}{\partial z}0,\quad \sigma_{zz}(\infty,t)=0,\quad \frac{\partial N(\infty,t)}{\partial z}=0, \tag{23}$$

$$\frac{\partial \mathrm{T}(0,t)}{\partial z}=-q_o,\quad \sigma_{zz}(0,t)=0,\quad \frac{\partial N(0,t)}{\partial z}=\gamma N(0,t),\quad \frac{\partial \mathrm{T}(\infty,t)}{\partial z}0,\quad \sigma_{zz}(\infty,t)=0,\quad \frac{\partial N(\infty,t)}{\partial z}=0, \tag{24}$$

where $u_1=\frac{n_o(3\lambda_o+2\mu_o)d_n}{(\lambda_o+2\mu_o)}$, $u_2=\frac{T_o(3\lambda_o+2\mu_o)\alpha_t}{(\lambda_o+2\mu_o)}$, $n_1=\frac{1}{\varsigma D_e}$, $\beta=\frac{\varepsilon T_o}{n_o\varsigma^2c^2D_e}$, $t_1=\frac{n_oE_{go}}{\rho c_eT_o}$, $t_2=\frac{(\lambda_o+2\mu_o)\alpha_t}{\rho_oc_e}$, and $\gamma=\frac{s_o}{\varsigma cD_e}$.

Exponential variation of nonhomogeneity

We take $f(z)=e^{-mz}$, where m is the non-dimensional constant. Then the Eqs. (18), (19), (20) and (21) reduce to

$$\frac{\partial^2u}{\partial z^2}-u_1\frac{\partial N}{\partial z}-u_2\frac{\partial T}{\partial z}-m\left(\frac{\partial u}{\partial z}-u_1N-u_2T\right)=\frac{\partial^2u}{\partial t^2}, \tag{25}$$

$$\frac{\partial^2N}{\partial z^2}-n_1\frac{N}{\tau}+\beta T=n_1\frac{\partial N}{\partial t}, \tag{26}$$

$$\frac{\partial^2T}{\partial z^2}-m\frac{\partial T}{\partial z}+\frac{t_1}{\tau}N-t_2\frac{\partial^2u}{\partial t\partial z}=\frac{\partial T}{\partial t} \tag{27}$$

$$\sigma_{zz}=e^{-mz}\left(\frac{\partial u}{\partial z}-u_1N-u_2T\right), \tag{28}$$

Laplace transform

The definition of Laplace transforms for any function $f(z,t)$ can be written as

$$\bar{f}(z,s)=L[f(z,t)]=\int_0^\infty f(z,t)e^{-st}dt,\ s>0 \tag{29}$$

where s is the Laplace's transform parameter. Thus, Eqs. (25)–(28) with the three cases of boundary conditions (22), (23) and (24) take the following forms:

$$\frac{d^2\bar{u}}{dz^2}-u_1\frac{d\bar{N}}{dz}-u_2\frac{d\bar{T}}{dz}-m\left(\frac{d\bar{u}}{dz}-u_1\bar{N}-u_2\bar{T}\right)=s^2\bar{u}, \tag{30}$$

$$\frac{d^2\bar{N}}{dz^2}-n_1\frac{\bar{N}}{\tau}+\beta\bar{T}=sn_1\bar{N}, \tag{31}$$

$$\frac{d^2\bar{T}}{dz^2}-m\frac{d\bar{T}}{dz}+\frac{t_1}{\tau}\bar{N}-st_2\frac{d\bar{u}}{dz}=s\bar{T} \tag{32}$$

$$\bar{\sigma}_{zz}=e^{-mz}\left(\frac{d\bar{u}}{dz}-u_1\bar{N}-u_2\bar{T}\right), \tag{33}$$

$$\frac{d\bar{\mathrm{T}}(0,s)}{dz}=\frac{-q_ot_p}{8(st_p+1)^3},\quad \bar{\sigma}_{zz}(0,s)=0,\quad \frac{d\bar{\mathrm{N}}(0,s)}{dz}=\gamma\bar{\mathrm{N}}(0,s),\quad \frac{d\bar{\mathrm{T}}(\infty,s)}{dz}=0,\quad \bar{\sigma}_{zz}(\infty,s)=0,\quad \frac{d\bar{\mathrm{N}}(\infty,s)}{dz}=0, \tag{34}$$

$$\frac{d\bar{\mathrm{T}}(0,s)}{dz}=\frac{-sq_o}{\omega^2+s^2},\quad \bar{\sigma}_{zz}(0,s)=0,\quad \frac{d\bar{\mathrm{N}}(0,s)}{dz}=\gamma\bar{\mathrm{N}}(0,s),\quad \frac{d\bar{\mathrm{T}}(\infty,s)}{dz}=0,\quad \bar{\sigma}_{zz}(\infty,s)=0,\quad \frac{d\bar{\mathrm{N}}(\infty,s)}{dz}=0, \tag{35}$$

$$\frac{d\bar{\mathrm{T}}(0,s)}{dz}=-\frac{q_o}{s},\quad \bar{\sigma}_{zz}(0,s)=0,\quad \frac{d\bar{\mathrm{N}}(0,s)}{dz}=\gamma\bar{\mathrm{N}}(0,s),\quad \frac{d\bar{\mathrm{T}}(\infty,s)}{dz}=0,\quad \bar{\sigma}_{zz}(\infty,s)=0,\quad \frac{d\bar{\mathrm{N}}(\infty,s)}{dz}=0, \tag{36}$$

Now, let us proceed to solve the homogeneous coupled differential Eqs. (30), (31) and (32) by the eigenvalues method which proposed [18–22]. Eqs. (30)–(32) can be rewritten in matrix-vector differential equations as follow

$$\frac{dV}{dz}=AV, \tag{37}$$

where V= $\left[\bar{u}\ \ \bar{N}\ \ \bar{T}\ \ \frac{d\bar{u}}{dz}\ \ \frac{d\bar{N}}{dz}\ \ \frac{d\bar{T}}{dz}\right]^T$ and

$$A=\begin{bmatrix}0&0&0&1&0&0\\0&0&0&0&1&0\\0&0&0&0&0&1\\a_{41}&a_{42}&a_{43}&a_{44}&a_{45}&a_{46}\\0&a_{52}&a_{53}&0&0&0\\0&a_{62}&a_{63}&a_{64}&0&a_{66}\end{bmatrix},$$

with $a_{41}=s^2$, $a_{42}=-mu_1$, $a_{43}=-mu_2$, $a_{44}=m$ $a_{45}=u_1$, $a_{46}=u_2$, $a_{52}=u_3\left(s+\frac{1}{\tau}\right)$, $a_{53}=-\beta$, $a_{62}=-\frac{t_1}{\tau}$, $a_{63}=s$, $a_{64}=t_2$, $a_{66}=m$.

After that, the characteristic equation of the matrix A can be given as

$$\xi^6+R_1\xi^5+R_2\xi^4+R_3\xi^3+R_4\xi^2+R_5\xi+R_6=0, \tag{38}$$

$$R_1=-a_{44}-a_{66},$$

$$R_2=-a_{41}-a_{52}-a_{63}-a_{46}a_{64}+a_{44}a_{66},$$

$$R_3=a_{44}a_{52}+a_{44}a_{63}-a_{43}a_{64}+a_{41}a_{66}+a_{52}a_{66},$$

$$R_4=a_{41}a_{52}-a_{53}a_{62}+a_{41}a_{63}+a_{52}a_{63}+a_{46}a_{52}a_{64}-a_{45}a_{53}a_{64}-a_{44}a_{52}a_{66},$$

$$R_5=a_{44}a_{53}a_{62}-a_{44}a_{52}a_{63}+a_{43}a_{52}a_{64}-a_{42}a_{53}a_{64}-a_{41}a_{52}a_{66},$$

$$R_6=a_{41}a_{53}a_{62}-a_{41}a_{52}a_{63},$$

The characteristic Eq. (38) has roots that, are also the eigenvalues of matrix A are of the form ξ_i, $i=1,2,\ldots,6$. The eigenvectors $Y=[Y_1,Y_2,Y_3,Y_4,Y_5,Y_6]$ corresponds to eigenvalues ξ can be computed by:

$$Y=\begin{pmatrix}a_{53}a_{62}-(-\xi^2+a_{52})(a_{63}+\xi(-\xi+a_{66}))\\-\xi a_{53}a_{64}\\\xi(a_{52}-\xi^2)a_{64}\\\xi(a_{53}a_{62}-(-\xi^2+a_{52})(a_{63}+\xi(-\xi+a_{66})))\\-\xi^2a_{53}a_{64}\\\xi^2(a_{52}-\xi^2)a_{64}\end{pmatrix}, \tag{39}$$

Using Eq. (39) the eigenvector Y corresponding to eigenvalue ξ_j, $j=1,2,3,4,5,6$ easily calculated. The general solutions of Eqs. (37) take following from:

$$\mathrm{V}(z,s)=\sum_{i=1}^{6}B_iY_ie^{-\xi_iz}, \tag{40}$$

where B_i, $i=1,2,\ldots6$ are constants that shown based on the boundary condition of the problem for three cases. Thus, the general solutions of the field variables for z and s were given below:

$$\bar{\mathrm{u}}(z,s)=\sum_{i=1}^{6}B_iU_ie^{-\xi_iz}, \tag{41}$$

$$\bar{\mathrm{N}}(z,s)=\sum_{i=1}^{6}B_iN_ie^{-\xi_iz}, \tag{42}$$

$$\bar{\mathrm{T}}(z,s)=\sum_{i=1}^{6}B_iT_ie^{-\xi_iz}, \tag{43}$$

$$\bar{\sigma}_{zz}(z,s)=-\sum_{i=1}^{3}B_i(\xi_iU_i+u_1N_i+u_2T_i)e^{-(\xi_i+m)z}, \tag{44}$$

To obtain the final solution for the distributions of displacement, carriers density, temperature and stress, the method of numerical inversion was adopted based on the Riemann-sum approximation method is used to observe the numerically results. In such a method, a function in the Laplace domain were transfored to the time domain as:

$$V(z,t)=\frac{e^{mt}}{t}\left(\frac{1}{2}Re[\overline{V}(z,m)]+Re\sum_{n=0}^{N}(-1)^{n}\overline{V}\left(z,m+\frac{in\pi}{t}\right)\right),\tag{45}$$

where i is the imaginary number unit and Re is the real part. Numerically experiments decided that $m=\frac{4.7}{t}$ in the case of faster convergence, that satisfies equation [23].

Numerical results and discussion

Now, to discuss the above phenomena numerically and shows the theoretical results, the silicon (Si) medium is considered. All parameters in this problem considered in SI. If the semiconductor is isotropic and the silicon sample was considered, the physical constants can be written as [10]:

$$\mu_o=5.46\times10^{10}\,(\mathrm{N})(\mathrm{m}^{-2}),\quad \lambda_o=3.64\times10^{10}\,(\mathrm{N})(\mathrm{m}^{-2}),\quad \rho_o=2330\,(\mathrm{kg})(\mathrm{m}^{-3}),\quad \tau=10^{-5}\,(\mathrm{s}),$$

$$c_e=695\,(\mathrm{J})(\mathrm{kg}^{-1})(\mathrm{k}^{-1}),\quad \alpha_t=3\times10^{-6}\,(\mathrm{k}^{-1}),\quad T_o=300\,(\mathrm{k}),\quad d_n=-9\times10^{-31}\,(\mathrm{m}^3),$$

$$s_o=2\,(\mathrm{m})(\mathrm{s}^{-1}),\quad E_{go}=1.11\,(\mathrm{eV}),\quad D_e=2.5\times10^{-3}\,(\mathrm{m}^2)(\mathrm{s}^{-1}),\quad n_o=10^{20}\,(\mathrm{m}^{-3}).$$

Based on the data set, Figs. 1–12 represent the numerically computed physical quantities at different values of the distance z. Numerical computations are carried out for the temperature, the carrier density, the distributions of both stress and displacement along the z-axis in the context of coupled photo-thermal theory.

For case (i) the surface ($z=0$) is exposed to a laser-pulse heat flux, Figs. 1–4 represents the three curves predicted by different values of non-homogeneous parameter m. From Fig. 1 it was noted that, the temperature begins by its maxima at $z=0$ and gradually reduces with raises the distance z up to zero beyond a wave front for the theory of photothermal, that satisfies our theoretical boundary conditions. Fig. 2 represents the variation of carrier density as a function of to the distance z. It is noticed that the carrier density values are some highest values on $z=0$ and reduces with the raising the distance z to close to zeros values. The displacement changes versus z are shown in Fig. 3. It was observed that the displacement shows an ultimate negative value then it raises gradually up to it attains a peak value at a location proximately nearby the surface then, its progressively decreases to zero. The changes of stress versus distance z at various times are shown as in Fig. 4. It is noticed that, the stress permanently starts by zero value and terminates at the zero obeying the boundary conditions. In compression between the solutions, it was found that, the non-homogeneous parameter is important phenomena and it was influence on the variations of field quantities. The photo-thermo-elastic responses in the non-homogeneity semiconducting medium are mainly dependent on non-homogeneity properties of medium. Therefore, one can design the property of non-homogeneity m for non-homogeneity structures to reduce the amplitude of heat stress in order to satisfy different engineering applications. Figs. 5–8 show the effects of non-homogeneity m in the physical quantities when the surface ($z=0$) is exposed to a transient cosine heat flux while Figs. 9–12 display the variations of physical quantities in the case of the surface ($z=0$) is exposed to a constant heat flux.

Acknowledgement

This project was funded by the Deanship of Scientific Research (DSR) at King Abdulaziz University, Jeddah, under grant no. (G: 229-130-1439). The authors, therefore, acknowledge with thanks DSR for technical and financial support.

References

[1] Todorović D. Photothermal and electronic elastic effects in microelectromechanical structures. Rev Sci Instrum 2003;74(1):578–81.
[2] Todorović D. Plasma, thermal, and elastic waves in semiconductors. Rev Sci Instrum 2003;74(1):582–5.
[3] Song Y, et al. Study of photothermal vibrations of semiconductor cantilevers near the resonant frequency. J Phys D Appl Phys 2008;41(15):155106.
[4] McDonald FA, Wetsel Jr GC. Generalized theory of the photoacoustic effect. J Appl Phys 1978;49(4):2313–22.
[5] Jackson W, Amer NM. Piezoelectric photoacoustic detection: theory and experiment. J Appl Phys 1980;51(6):3343–53.
[6] Stearns R, Kino G. Effect of electronic strain on photoacoustic generation in silicon. Appl Phys Lett 1985;47(10):1048–50.
[7] Rosencwaig A, Opsal J, Willenborg DL. Thin-film thickness measurements with thermal waves. Appl Phys Lett 1983;43(2):166–8.
[8] Opsal J, Rosencwaig A. Thermal and plasma wave depth profiling in silicon. Appl Phys Lett 1985;47(5):498–500.
[9] Song Y, et al. Study on the generalized thermoelastic vibration of the optically excited semiconducting microcantilevers. Int J Solids Struct 2010;47(14):1871–5.
[10] Song Y, et al. Bending of semiconducting cantilevers under photothermal excitation. Int J Thermophys 2014;35(2):305–19.
[11] Song Y, Bai J, Ren Z. Reflection of plane waves in a semiconducting medium under photothermal theory. Int J Thermophys 2012;33(7):1270–87.
[12] Song Y, Bai J, Ren Z. Study on the reflection of photothermal waves in a semiconducting medium under generalized thermoelastic theory. Acta Mech 2012;223(7):1545–57.
[13] Abbas IA, Aly K. A study on photothermal waves in a semiconductor material photogenerated by a focused laser beam. J Mol Eng Mater 2016;4(02):1650003.
[14] Abbas IA. A dual phase lag model on photothermal interaction in an unbounded semiconductor medium with cylindrical cavity. Int J Comput Mater Sci Eng 2016;5(03):1650016.
[15] Abbas IA, Aly K. A generalized model on plasma, thermal and elastic waves in a semiconductor medium. J Adv Phys 2017;6(3):317–25.
[16] Abbas IA, Aly K, Alzahrani FS. A two-temperature photothermal interaction in a semiconducting material. J Adv Phys 2017;6(3):402–7.
[17] Mandelis A, Nestoros M, Christofides C. Thermoelectronic-wave coupling in laser photothermal theory of semiconductors at elevated temperatures. Opt Eng 1997;36(2):459–68.
[18] Das NC, Lahiri A, Giri RR. Eigenvalue approach to generalized thermoelasticity. Indian J Pure Appl Math 1997;28(12):1573–94.
[19] Abbas IA. Eigenvalue approach in a three-dimensional generalized thermoelastic interactions with temperature-dependent material properties. Comput Math Appl 2014;68(12):2036–56.
[20] Abbas IA. Eigenvalue approach for an unbounded medium with a spherical cavity based upon two-temperature generalized thermoelastic theory. J Mech Sci Technol 2014;28(10):4193–8.
[21] Abbas IA. A dual phase lag model on thermoelastic interaction in an infinite fiber-reinforced anisotropic medium with a circular hole. Mech Based Des Struct Mach 2015;43(4):501–13.
[22] Abbas IA. The effects of relaxation times and a moving heat source on a two-temperature generalized thermoelastic thin slim strip. Can J Phys 2015;93(5):585–90.
[23] Tzou DY. Macro-to micro-scale heat transfer: the lagging behavior. CRC Press; 1996.